Isı Bilimi ve Tekniği Dergisi, 33, 2, 125-133, 2013
J. of Thermal Science and Technology

ISSN 1300-3615

DETERMINATION OF TRANSITION ONSET IN LAMINAR PULSATILE PIPE FLOWS

Emrah ÖZAHİ* and Melda Özdinç ÇARPINLIOĞLU*

*Department of Mechanical Engineering, University of Gaziantep, 27310, Gaziantep, Turkey
ozahi@gantep.edu.tr, melda@gantep.edu.tr

(Geliş Tarihi:16.03.2012 Kabul Tarihi:27.07.2012)

Abstract: This paper presents a program devised in LabView 2009SP1® for the detection of the transition onset in laminar pulsatile pipe flows. As a conclusion of a comprehensive literature survey, it is deduced that there is no well-defined detection program even a methodology for determination of transition onset besides of conventional methods of visual observation on velocity waveforms. The operation of the program which is an original contribution to literature is introduced giving sample plots in the range of time-averaged Reynolds number of 1019±35 ≤ Re_{ta} ≤ 4817±164, oscillating Reynolds number of 107±4 ≤ Re_{os} ≤ 4261±145, velocity amplitude ratio of 0.05±0.0017 ≤ A_l ≤ 0.96±0.03 and Womersley number of 2.72 ≤ $\sqrt{\omega'}$ ≤ 32.21. As an original contribution to the available literature, two different flow maps that identify the border between laminar flow and transition onset in pulsatile pipe flow in terms of $Re_{ta}= Re_{ta}(Re_{os})$ and $Re_{ta}= Re_{ta}(\sqrt{\omega'})$ are introduced in the covered experimental ranges.
Keywords: LabView, Turbulence Detection, Laminar to Turbulent Transition, Womersley Number, Pulsatile Pipe Flow.

LAMİNAR DARBELİ BORU AKIŞLARINDA GEÇİŞ BAŞLANGICININ BELİRLENMESİ

Özet: Bu makale laminar darbeli boru akışlarında türbülansa geçişin başlangıcının belirlenmesi için LabView2009SP1® de geliştirilmiş bir programı sunmaktadır. Detaylı bir literatür taraması sonucunda, hız dalga formlarının görsel gözlemlenmesi gibi geleneksel bir yöntemden başka türbülansa geçiş başlangıcının belirlenmesi için tanımlanmış ne bir program ne de bir yöntembilimi olmadığı görüşüne varılmıştır. Literatüre önemli bir katkı olan programın işleyişi belirtilen zaman ortalamalı Reynolds sayısı; 1019±35 ≤ Re_{ta} ≤ 4817±164, salınımlı Reynolds sayısı; 107±4 ≤ Re_{os} ≤ 4261±145, hız genlik oranı; 0.05±0.0017 ≤ A_l ≤ 0.96±0.03 ve Womersley sayısı 2.72 ≤ $\sqrt{\omega'}$ ≤ 32.21 aralıklarında örnek grafikler verilerek tanıtılmaktadır. Mevcut literatüre orijinal bir katkı olarak, tanımlanan deney aralıkları içerisinde, darbeli boru akışlarında laminar akım ile türbülansa geçişin başlangıcı arasındaki sınırı $Re_{ta}= Re_{ta}(Re_{os})$ ve $Re_{ta}= Re_{ta}(\sqrt{\omega'})$cinsinden belirleyen iki farklı akım haritası sunulmuştur.
Anahtar Kelimeler: LabView, Türbülans Belirlenmesi, Laminardan Türbülansa Geçiş, Womersley Sayısı, Darbeli Boru Akışı

NOMENCLATURE

A_l	velocity amplitude ratio $[=\lvert\overline{U}_{m,os,1}\rvert/\overline{U}_{m,ta}]$
D	pipe inner diameter [m]
f	frequency of oscillation [Hz]
r	radial position from centerline [m]
R	pipe radius [m]
Re_{os}	oscillating Reynolds number $[=\lvert\overline{U}_{m,os,1}\rvert D/\nu]$
Re_{ta}	time-averaged Reynolds number $[=\overline{U}_{m,ta}D/\nu]$
t	time coordinate [s]
u	characteristic velocity [m/s]
$U(r,t)$	instantaneous axial velocity [m/s]
$\lvert\overline{U}_{m,os,l}\rvert$	oscillating component of cross-sectional mean velocity [m/s]
$\overline{U}_{m,ta}$	time-averaged component of cross-sectional mean velocity [m/s]
$\overline{U}_{ta}$	time-averaged component of local velocity at any radial position of the probe [m/s]
X	axial length from the end of MFC unit [m]

Greek Letters

∂	partial derivative
ν	kinematic viscosity [m²/s]
ω	angular frequency of oscillation $[=2\pi f]$ [rad/s]
ω'	dimensionless frequency of oscillation $[=R^2\omega/\nu]$
$\sqrt{\omega'}$	Womersley number, $[=R\sqrt{\omega/\nu}]$

Abbreviates

MFC	mass flow control
subvi	sub virtual instrument
vi	virtual instrument in LabView

INTRODUCTION

Transition to turbulence in pulsatile pipe flows has been an ongoing research area since last century. There are many experimental studies conducted on the manner as mentioned in (Gündoğdu and Çarpınlıoğlu, 1999; Çarpınlıoğlu and Gündoğdu, 2001; Çarpınlıoğlu, 2003). However, the studies on the determination method of transition to turbulence are still in a very scarce amount.

There seems to be two separate approaches for the analyses of the experimental results on transition to turbulence. One of these approaches is related to the consideration of flow as quasi-steady flow and stresses the instantaneous values of the flow parameters, in particular Reynolds number and the existence of the inflection points on the velocity profile (Shemer, 1985). The alternative approach is based on the unsteady character of time-dependent flow which is subject to alternating acceleration and deceleration. However, the theoretical studies conducted on the linear stability of the time-dependent flows indicate that contrary to steady flows, the inflection points on the velocity profile does not affect the stability. Moreover, it is declared that superimposing of oscillation on the steady flow has a stabilizing effect at intermediate frequencies (Stettler et al., 1986; Einav and Sokolov, 1993; Peacock et al., 1998).

The studies related to transitional pulsatile pipe flows are based mainly on the observations of velocity waveforms and detection of disturbance growth. The detailed studies are seen in the early 1960's. The first study conducted on laminar to tur
bulent transition in a pulsatile pipe flow by means of flow visualization is one by Gilbrech and Combs (1963). Later, Sarpkaya (1966) carried out an experimental study for pulsatile Poiseuille flow of aero hydraulic oil. The flow remained laminar up to Reynolds number of 6500 above which random 3-D bursts of turbulence were observed. Yellin (1966) investigated the development of turbulence by analyzing the dynamic characteristics of the transition such as the velocity, growth rate and intermittency for a simple sinusoidal pulsatile pipe flow of dilute aqueous dispersion of bentonite. The flow was classified by means of visual observations as laminar, disturbed and turbulent flow. Another study for sinusoidal water pipe flow was performed by Hershey and Im (1968). The experimental friction factors with theoretical ones were compared, which gave an excellent agreement between them. The departure from the theory was estimated as the onset of the transition. Clamen and Minton (1977) measured the velocities and the intermittency of the periodic bursts of pulsatile water flow by means of the hydrogen-bubble technique. From the visual observation, the pulsatile flow was found to be undisturbed, disturbed or highly disturbed. Ohmi et al. (1982) observed the velocity waveforms on pulsatile air pipe flow and classified the flow near the transition region into three types as laminar, disturbed with small amplitude perturbation in the early acceleration phase and turbulent flow with turbulent bursts occurring in the decelerating phase and over the full oscillation cycle. Previously, Ohmi et al. (1981) classified the flow pattern for a pulsatile laminar pipe flow into three types as quasi-steady ($\sqrt{\omega'}$ <1.32), intermediate (1.32< $\sqrt{\omega'}$ <28) and inertia dominant ($\sqrt{\omega'}$ >28) with respect to the dimensionless frequency parameter, $\sqrt{\omega'}$. Iguchi and Ohmi (1984) studied on transitional pulsatile pipe flow at $Re_{ta}<10^5$ and $Re_{os}<10^5$ and classified the flow into four categories as; laminar, transitional, conditionally turbulent and fully turbulent although pulsatile flows were classified into three regimes such as laminar, transitional and turbulent flows in their first report. Nabavi (2010) and Nabavi and Siddiqui (2010) reviewed the advanced velocity measurement techniques in pulsatile flows. They emphasized that there has recently been a growing interest in experimental pulsatile flow studies due to more improved measurement devices. Hotwire anemometer was found to have superior dynamic range and high spatial resolution for measurements in pulsatile flows. For more accurate point measurements, LDV was suggested. PIV was also found to be suitable for many time dependent pipe flows. As can be seen, transition to turbulence has generally been detected by visual observations on the velocity waveforms until now. Some illusions may be occurred during the detection of transition by visual observation. The method introduced herein is based on taking the derivative of velocity waveform with respect to time. By taking the derivative of time-dependent signal, its time-dependency is eliminated and if there is any perturbation on the signal due to transition onset, it can be easily detected as peaks on the derivative form of the velocity waveforms.

In this paper, we deal with the instant phenomenon of the laminar to turbulent transition denoted as the onset of transition to turbulence. An original devised method in LabView 2009SP1® for the detection of transition onset in pulsatile pipe flows is presented. The brief description of the experimental set-up, the used methodology and the details of the devised software program are introduced. The flow dynamics of transitional pulsatile pipe flow and the working principle of the method are presented giving some sample runs.

BRIEF DESCRIPTION OF THE EXPERIMENTAL SET-UP, UTILIZED METHODOLOGY AND DETAILS OF THE DEVISED SOFTWARE PROGRAM

Experimental Set-up

Pulsatile air flow through pipeline is generated by means of a screw air compressor in combination with a mass flow control (MFC) unit (Fig. 1). The experimental set-up is controlled automatically by means of a program devised in LabView2009SP1®environment. DANTEC

56C01 CTA, 55P11 type miniature-probe which is frequently calibrated during the experiment (Özahi et al., 2010) and RCP2-SA6-I-PM-6-200-P1-SBE coded Robo-cylinder traverse mechanism are used for the velocity measurement. The local static pressure measurements at seven downstream locations are performed by WIKA SL-1 pressure transmitters. A 16-bit, 1-MHz A/D converter IOtech Daq3001 USB board coupled to a PC is used for controlling of the MFC unit, acquisition of the raw data from DANTEC 56C01 CTA and WIKA SL-1transmitters with a sampling frequency of 100 Hz without any signal aliasing and any unnecessary data storage.

The instantaneous axial velocity at 13 radial positions at *X*/*D*=604 and the static pressures along the pipeline are measured simultaneously with an uncertainty of ±3% and ±1.3%, respectively. The characteristic parameters of pulsatile pipe flow of $\mathrm{Re}_{ta}, \mathrm{Re}_{os}$, $\sqrt{\omega'}$ and A_1 are changed systematically during the study. The details of the experimental set-up and the used methods can be found in (Özahi et al., 2010; Çarpınlıoğlu and Özahi, 2011; Özahi, 2011).

Utilized Methodology

In view of the literature survey, it is seen that the detection of turbulent structures is carried out by means of visual observation on velocity waveforms. However the visual observation is seen to be an elementary and open-ended method. It is not easy, sensitive and objective method giving rise to the possibility of human errors, i.e., visual illusions. Hence a method is developed and a fully-automated program is devised in LabView 2009SP1® in order to detect the transition onset in laminar pulsatile pipe flow.

The velocity profile $U = U(r,t)$ is considered to be used for the detection method. Taking the derivative of instantaneous velocity profile with respect to time, the time-periodicity is eliminated. Hence any perturbation in any frequency due to occurrence of transition onset can be noticed as a peak in $dU(r,t)/dt$. This parameter is defined as turbulence detection parameter, TDP as follows;

$$TDP_0 = dU(r,t)/dt \tag{1}$$

The detection method is based on the comparison of the turbulence detection parameter, TDP with a threshold parameter TP. Any TP should be defined as a comparison tool such that any value of TDP over the value of TP is the signature of any transition onset. In this respect, a value of TP_0 is defined and compared with $TDP_0 = dU(r,t)/dt$ in the devised program. However, the parameter of $TDP_0 = dU(r,t)/dt$ is found to be nonsense due to both positive and negative values of $dU(r,t)/dt$ appearing in the analysis, which require two different values of TP for both positive and negative values of $dU(r,t)/dt$ for comparison.

For this reason, $TDP_0 = dU(r,t)/dt$ is squared and defined as a new TDP eliminating the negative and magnifying the value as follows;

$$TDP_1 = \left(dU(r,t)/dt\right)^2 \tag{2}$$

Hence it becomes easier to detect very small perturbations on the velocity waveforms. It is seen that TDP_1 has been used as a turbulence detector also in the study of Shemer (1985) due to only axial component of the velocity has been measured in his study. However, it is observed that the parameter of $TDP_1 = \left(dU(r,t)/dt\right)^2$ with any value of TP_1 does not execute very well for the covered experimental ranges. It is found to be unsatisfactory for the detection of transition onset at some instants and radial positions of the hotwire probe, r/R although turbulent structures are seen on velocity waveforms.

Therefore, it is decided to define a new couple of TDP and TP such that the proposed method operates without any error and detects immediately transition onset when any turbulent structures occur on velocity waveforms at any instant and radial position of r/R. It is not reasonable to derive a TDP taking only the derivative of $U(r,t)$ with respect to time in order to propose a unique TDP that covers all experimental range. Hence, the varying parameters such as a flow parameter of time-averaged component of local velocity at any radial position, $\overline{U}_{ta}$, an unsteady parameter of angular frequency, ω, which covers the effect of oscillation frequency, f ($\omega = 2\pi f$), a fluid property of kinematic viscosity, ν, and a physical characteristic of the pipe which may be radius, *R*, should be taken into consideration. Therefore, TDP should be a function of $\overline{U}_{ta}$, R, ν and f. Using the dimensional analysis, the following expression is derived as follows;

$$TDP_2 = \left[R\left(dU(t)/dt\right)^2\right] / \left[\overline{U}_{ta}\nu\omega^2\right] \tag{3}$$

TDP_2 is a non-dimensional and dynamic parameter as a function of $\overline{U}_{ta}$, R, ν, f and $dU(r,t)/dt$. Hence, its value changes at any instant and radial position, r/R. As a comparison tool, a new non-dimensional and dynamic TP is derived, whose magnitude is changed with varying of f, as follows;

$$TP_2 = \left(1/\sqrt{\omega'}\right)^f \tag{4}$$

As a result of the extended tests, the method based on the comparison of TDP_2 and TP_2 is found to be accurate and effectiveness for the detection of transition onset. The value of TDP_2 at any instant exceeds the value of TP_2 when turbulent structures occur on the velocity waveform at any radial position. The intermittency factor, γ (as a ratio of the time period during the occurrence of

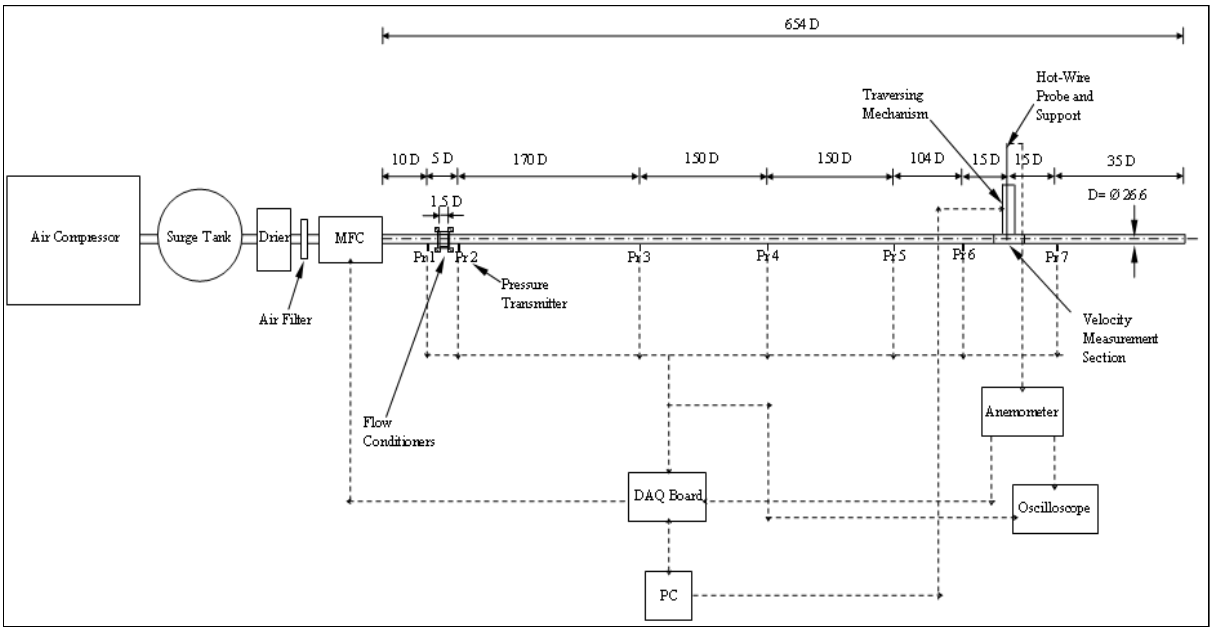

Figure 1. A schematic layout of the experimental set-up.

turbulence structures to the total time period) at transition onset is found to be less than 0.1 in the covered experimental ranges. At that moment, the related devised program detects simultaneously the transition onset and gives an alert. In laminar regime, however, the value of TP_2 is always observed to be above the value of TDP_2, which results that the program does not give any alert.

However, it is observed that the method does not work well for f >1 Hz. At some instants, the program cannot detect available turbulent structures on velocity waveforms for f >1 Hz. For this reason, the program is divided into two parts for the cases of f≤1 Hz and f >1 Hz and it becomes essential to define a new couple of TDP and TP for f >1 Hz. As a conclusion of the related literature, it is known that the flow at almost f >1 Hz ($\sqrt{\omega'}$ =8.61) approaches to the inertia dominant regime. Therefore the dominant term in TDP should be the velocity term instead of a viscous term. For this reason, a new couple of TDP and TP are derived for f >1 Hz as follows;

$$TDP_3 = \left[(dU(t)/dt)^2 \right] / \left[\overline{U}_{ta}^2 \omega^2 \right] \qquad (5)$$

$$TP_3 = \left(1/\sqrt{\omega'} \right)^4 \qquad (6)$$

In this form of $TDP_3 = \left[(dU(t)/dt)^2 \right] / \left[\overline{U}_{ta}^2 \omega^2 \right]$, the viscous term, ν is not seen. Moreover, the square of the inertia term, $\overline{U}_{ta}$ is dominant. This verifies that, after f >1 Hz, the flow regime approaches nearer to the inertia dominant regime defined previously by Ohmi and Iguchi (1980) and Ohmi et al. (1982). The new proposed TDP_3 and TP_3 are found to be accurate and effectiveness for transition onset determination at f >1 Hz.

Figs. 2 and 3 show the variation of the dynamic $TP_2 = \left(1/\sqrt{\omega'} \right)^f$ and $TP_3 = \left(1/\sqrt{\omega'} \right)^4$ for f ≤1 Hz and f >1 Hz, respectively. The values of TP_2 and TP_3 decrease when $\sqrt{\omega'}$ increases, however the characteristics of the variations are quite different from each other.

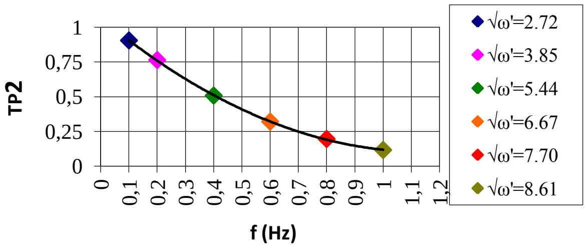

Figure 2. Variation of TP_2 with f in the range of 2.72≤ $\sqrt{\omega'}$ ≤8.61

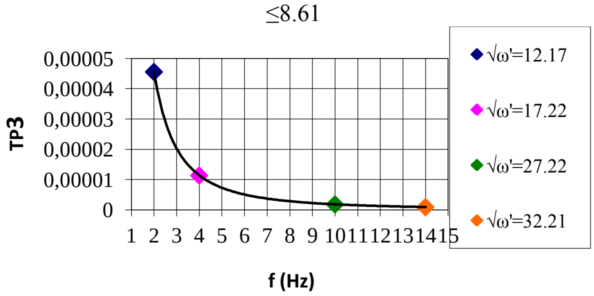

Figure 3. Variation of TP_3 with f in the range of 12.17≤ $\sqrt{\omega'}$ ≤32.21

Details of the Devised Software Program

Using the utilized methodology mentioned in the previous section, the turbulence detection program is devised and embedded into the main flow control program which is used for the generation, control and analyses of time-dependent pipe flows. The block diagrams of the detection program are given in Figs. 4(a) and 4(b).

In the *Case Structure* (5), the detection of transition onset is performed. On the left hand side of the *Case Structure*, there is a *Comparison Palette* named as *Less Or Equal*. The frequency of oscillation, *f*, is wired to this comparison palette. The output of the comparison palette is wired to the selector of the *Case Structure*. If $f \leq 1$ Hz, the *True* case of the structure executes. If not, the *False* case of the structure executes.

As can be seen from Fig. 4(a), the mathematical code of the dynamic *TDP* is constructed in the form of $TDP_2 = \left[R(dU(t)/dt)^2\right] / \left[\overline{U}_{ta}\nu\omega^2\right]$ using *Compound Arithmetic* and *Numeric palettes*. The numeric values of $TDP_2 = \left[R(dU(t)/dt)^2\right] / \left[\overline{U}_{ta}\nu\omega^2\right]$ are converted to dynamic values by means of the signal manipulation palette named as *Convert to Dynamic Data*. The dynamic values of $TDP_2 = \left[R(dU(t)/dt)^2\right] / \left[\overline{U}_{ta}\nu\omega^2\right]$ is then transferred to *Amplitude and Level Measurements.vi*. In this subvi, the maximum peak value of TDP_2 is determined. On the other hand, the dynamic $TP_2 = \left(1/\sqrt{\omega'}\right)^f$ is constructed in the block diagram by means of *Power Of X* palette.

Using the *Threshold Peak Detector.vi*, the values of $TDP_2 = \left[R(dU(t)/dt)^2\right] / \left[\overline{U}_{ta}\nu\omega^2\right]$ that exceed the value of $TP_2 = \left(1/\sqrt{\omega'}\right)^f$ are detected. If the number of these values is greater than five and if the maximum peak value of TDP_2 is greater than the value of TP_2, the program gives an alert as "*Transition Detected*". At that moment, the indicator on the front panel of the program gives an alarm and the lamp lights.

If $f > 1$ Hz, the *False* case of the structure executes and the same operations are performed for $f > 1$ Hz to detect whether transition onset occurs or not in the structure of *False* case. For $f > 1$ Hz, *TDP* and *TP* become as $TDP_3 = \left[(dU(t)/dt)^2\right] / \left[\overline{U}_{ta}^2\omega^2\right]$ and $TP_3 = 1/\sqrt{\omega'}^4$, respectively as seen in Fig. 4(b).

If transition to turbulence is detected at any time of the velocity waveform and radial positions through the half of the pipe cross-section, the green lamp on the front panel lights and it gives an alert. At that moment, all raw and processed data in corresponding run are saved in a file named automatically as "(Transitional Regime) Re_{ta} =...; Re_{os} =...; fre=...;wom=...". If no transition to turbulence is detected at any radial position of the hotwire probe, the data are saved in a file only named as " Re_{ta} =...; Re_{os} =...;fre=...;wom=.."

RESULTS AND DISCUSSION

The devised transition onset detection method is tested and its accuracy, functionality and effectiveness are verified in the covered experimental ranges. In reference to the experimental test cases covered, the following deductions can be listed below as;

i) The instantaneous velocity waveforms corresponding to the run at Re_{ta} =2805±95, Re_{os} =2001±68, $\sqrt{\omega'}$ =2.72 and A_1=0.71±0.024 for all *r/R* radial positions and for one period are given in Fig 5. As can be seen from the figure, the transition onset occurs at the decelerating phases of the velocity waveform for all *r/R* radial positions as denoted in the literature (Gündoğdu and Çarpınlıoğlu, 1999; Çarpınlıoğlu and Gündoğdu, 2001; Stettler and Hussain, 1986; Eninav and Sokolov, 1993; Peacock et al., 1998; Ohmi and Iguchi, 1980; Ohmi et al., 1982).

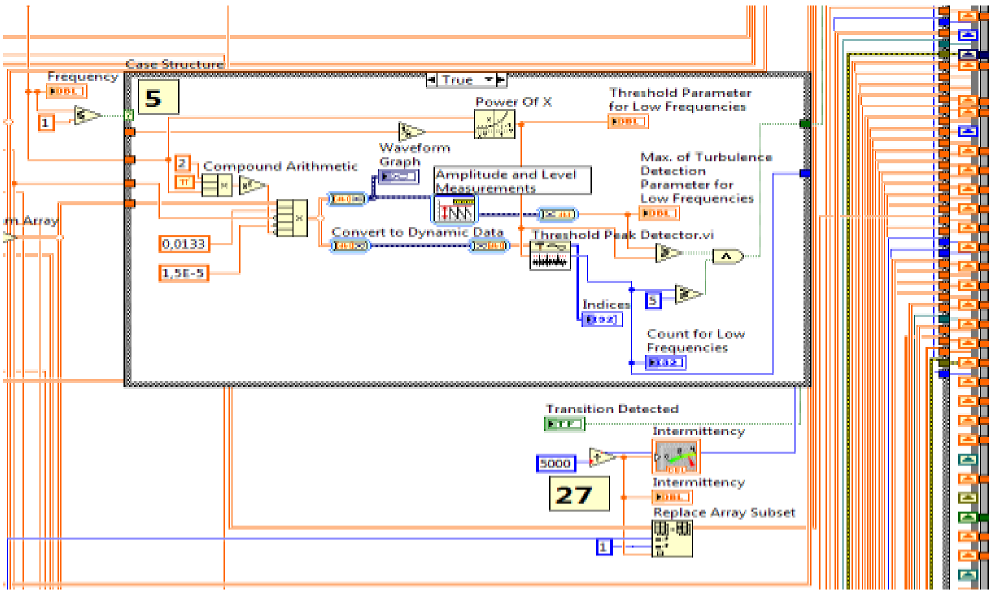

Figure 4(a). A first "True" section of the turbulence detection program for $f \leq 1$ Hz

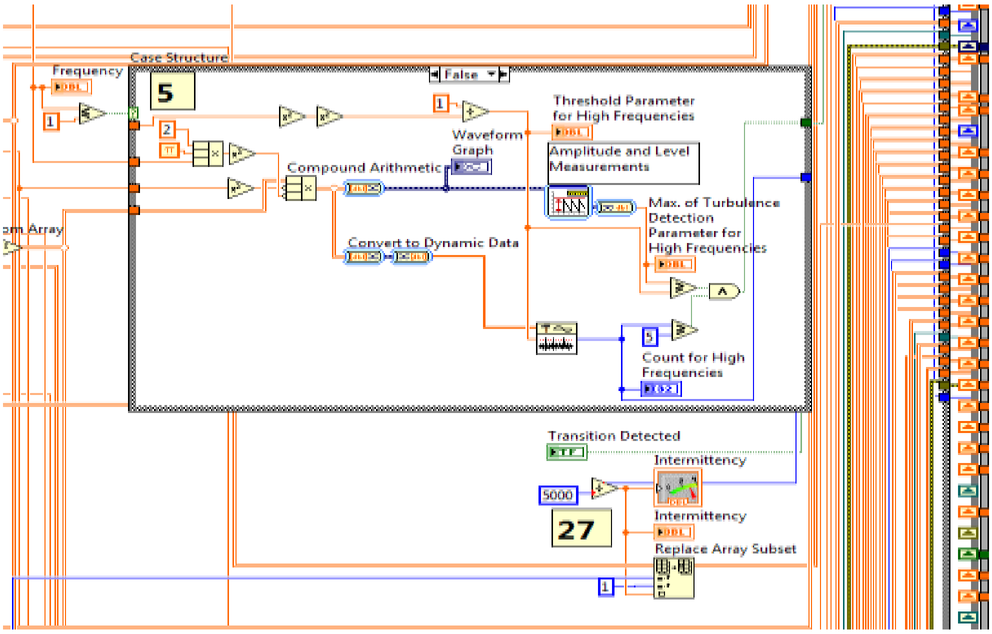

Figure 4(b). A second "False" section of the turbulence detection program for f >1 Hz

ii) It is seen that the transition onset is always seen in the decelerating phase of the velocity waveform for all runs in the study irrespective of the magnitudes of A_1 and $\sqrt{\omega'}$.

iii) Figures 6 and 7 show the one-period velocity waveforms for the same run at r/R=0 (centerline) and r/R=0.977 (nearer the pipe wall), respectively. As is seen from the figures, the shape of the velocity waveforms at the transition onset is dependent on r/R. The shape of the velocity waveforms at $r/R \leq 0.692$ have a collapsing part followed by small scale perturbations (Fig. 6) while the ones taken at r/R>0.692 have a peak (Fig. 7), which are same as observed structures in the papers of (Shemer, 1985; Stettler and Hussain, 1986; Ohmi and Iguchi, 1980; Ohmi et al., 1982).

iv) Figure 8 illustrates the graphical results of the method for the flow regime at Re_{ta} =2805±95, Re_{os} =2001±68, $\sqrt{\omega'}$ =2.72 and A_1 =0.71±0.024 at r/R=0 and r/R=0.977. For this run, the first part of the detection program executes due to the oscillation frequency being f=0.1 Hz.

Therefore TDP and TP become as $TDP_2 = \left[R(dU(t)/dt)^2\right] / \left[\bar{U}_{ta} \nu \omega^2\right]$ and $TP_2 = \left(1/\sqrt{\omega'}\right)^f$, respectively. For f = 0.1 Hz, the value of TP_2 is evaluated by the devised program as $TP_2 = \left(1/\sqrt{\omega'}\right)^f = (1/2.72)^{0.1} = 0.905$ which is illustrated with the dotted line on the plots. As can be seen from Fig. 8, there are peaks on the plots which represent the transition onset. The values of TDP_2 at these peaks are greater than the values of TP_2=0.905 at r/R=0 and r/R=0.977. Hence the program detects the transition onset at these radial positions. The transition to turbulence corresponding to this run has been previously seen in Figs.5-7. Hence the corresponding run is fully transitional due to the detection of the transition onset at all r/R as seen in Fig. 5.

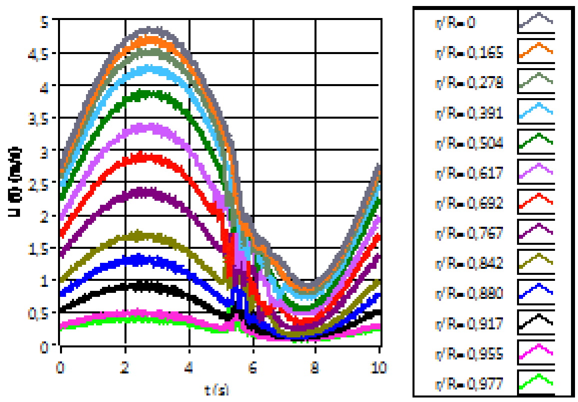

Figure 5. Instantaneous velocity waveforms at all r/R positions at Re_{ta} =2805±95, Re_{os} =2001±68, $\sqrt{\omega'}$ =2.72 and A_1 =0.71±0.024

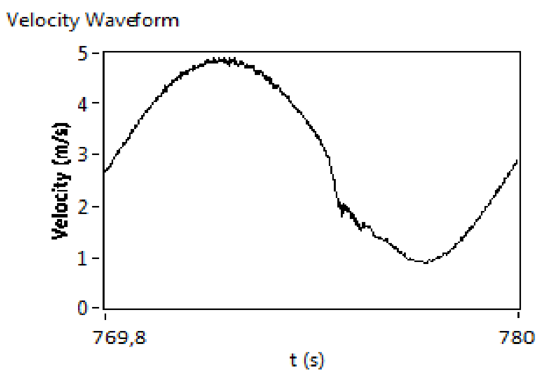

Figure 6. Local velocity waveforms at r/R=0 for one period at Re_{ta} =2805±95, Re_{os} =2001±68, $\sqrt{\omega'}$ =2.72 and A_1 =0.71±0.024

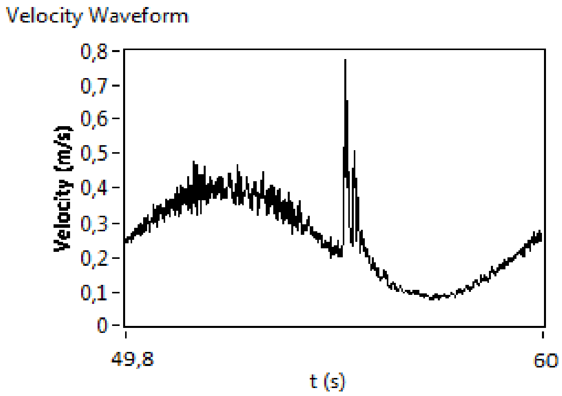

Figure 7. Local velocity waveforms at r/R=0.977 for one period at Re_{ta} =2805±95, Re_{os} =2001±68, $\sqrt{\omega'}$ =2.72 and A_1 =0.71±0.024

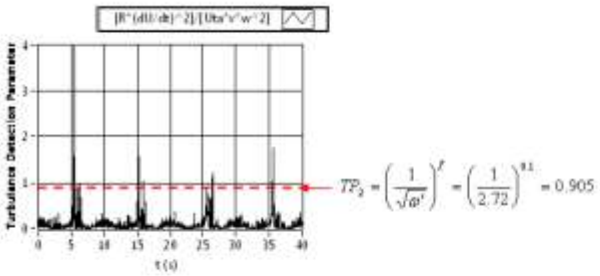

(a) r/R=0

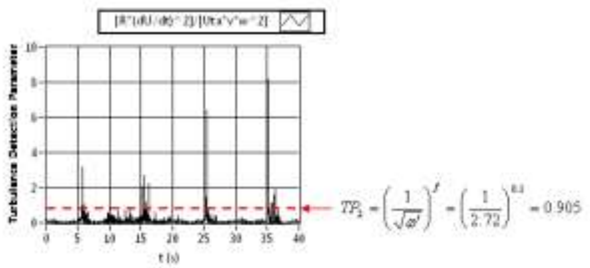

(b) r/R=0.977

Figure 8. Variation of dynamic turbulence detection parameter at r/R=0 and r/R=0.977 at Re_{ta} =2805±95, Re_{os} =2001±68, $\sqrt{\omega'}$ =2.72 and A_1 =0.71±0.024

v) As is noticed from Fig. 8, the occurrence of the transition to turbulence has also time-periodicity, due to the propagations of the turbulent structures to downstream of the pipeline. The peaks appear at the definite time period, i.e. almost at t=6 s, 16 s, 26 s and 36 s at both r/R=0 and r/R=0.977 with the incremental of 10 s which belongs to the period of T=10 s for f=0.1 Hz.

vi) The devised program then saves automatically all raw and processed data, the corresponding charts and graphs related to this run to the file named as "(Transitional Regime) Re_{ta} =2805; Re_{os} =2001; fre=0.10;wom=2.72".

vii) Figure 9 shows the output of the detection method for the laminar flow regime at Re_{ta} =2160±73, Re_{os} =832±28, $\sqrt{\omega'}$ =17.22 and A_1 =0.39±0.013 for r/R=0 and r/R=0.977. The corresponding oscillation frequency, f, with respect to $\sqrt{\omega'}$ =17.22 is 4 Hz. Therefore, the second part of the detection program executes. The dynamic *TDP* and *TP* are shown on the plot as $TDP_3 = \left[(dU(t)/dt)^2\right] / \left[\overline{U}_{ta}^2 \omega^2\right]$ and $TP_3 = 1 / \sqrt{\omega'}^4$, respectively. For f=4 Hz ($\sqrt{\omega'}$ =17.22), the value of TP_3 is evaluated as $\left(1/\sqrt{\omega'}\right)^4 = (1/17.22)^4 = 11.3*10^{-6}$ specified with the dotted line**.** However, the values of TDP_3 at any instant at r/R=0 and r/R=0.977 are less than the value of $TP_3 = 11.3*10^{-6}$. Hence no transition to turbulence is detected on the velocity waveform at r/R=0 and r/R=0.977 by the devised detection program. Moreover, the corresponding local velocity waveforms for this run are given in Fig. 10 at all r/R for one period. As can be seen, transition to turbulence is also not observed at any r/R on the waveform graph contrary to Fig. 5 verifying the detection program.

viii) In the experiment, it is exactly observed that transition to turbulence is detected firstly near the pipe wall at r/R=0.977 for all runs and whether it propagates to the center of the pipe *(r/R*=0) or disappears before reaching the pipe centerline.

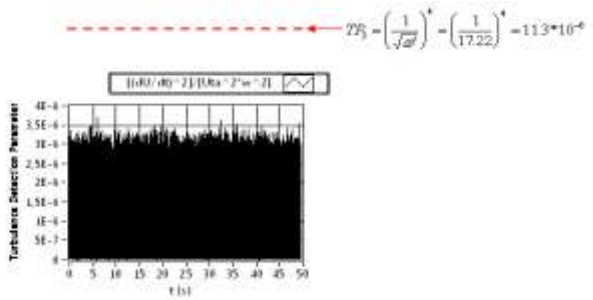

(a) r/R=0

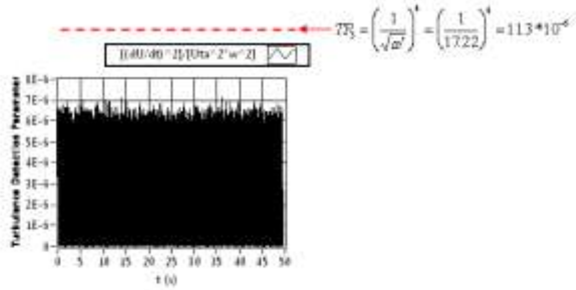

(b) r/R=0.977

Figure 9. Variation of dynamic turbulence detection parameter at r/R=0 and r/R=0.977 at Re_{ta} =2160±73, Re_{os} =832±28, $\sqrt{\omega'}$ =17.22 and A_1 =0.39±0.013

ix) The non-dimensional parameters of Re_{ta}, Re_{os} and $\sqrt{\omega'}$ are calculated using all experimental data. The relationships of Re_{ta} versus Re_{os} and Re_{ta} versus $\sqrt{\omega'}$ are specified and these are plotted on the graph, which are defined as "Flow Maps". Figure 11 shows the results

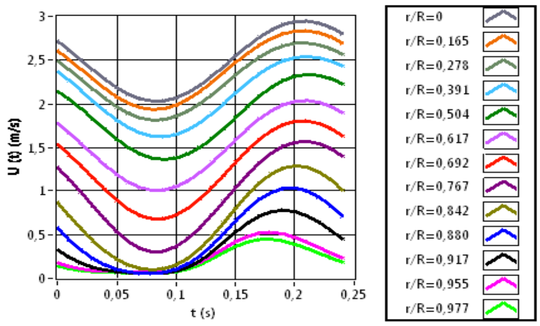

Figure 10. Local velocity waveforms at all r/R for one period at Re_{ta} =2160±73, Re_{os} =832±28, $\sqrt{\omega'}$ =17.22 and A_1 =0.39±0.013

of the analyses giving a flow map for the region of laminar and onset of transitional regime in the covered experimental range. "L" and "OT" denote laminar regime and onset of transition, respectively. As seen from the figure, the transition to turbulence starts when Re_{ta} is above roughly $\mathrm{Re}_{ta,crit}$ =2700. Below this value, the flow is seen to be laminar. Hence this figure gives an overall idea about the region between the laminar regime and the onset of transition in the covered range. Besides, the flow can be maintained as laminar at higher Re_{ta} in the order of nearly 3500 at $\sqrt{\omega'}$ =3.85 (f=0.2 Hz). Hence these data of Re_{ta} =3696, Re_{ta} =3803 and Re_{ta} =3058 in which the flow is still laminar at $\sqrt{\omega'}$ =3.85 (f=0.2 Hz) are above the border of critical state of $\mathrm{Re}_{ta,crit}$ ≈2700, which are circled in the figure.

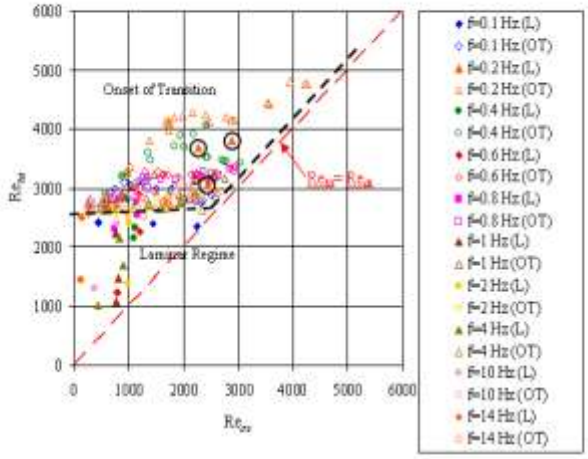

Figure 11. Flow map showing laminar regime and the onset of transition in terms of Re_{ta} and Re_{os}

Figure 12 shows the critical limit between the laminar regime and the onset of transition to turbulence in the range of 2.72≤ $\sqrt{\omega'}$ ≤32.21. The overall characteristic of the relationship between $\mathrm{Re}_{ta,crit}$ and $\sqrt{\omega'}$ is given with the dashed line. It can be deduced that the behavior of $\mathrm{Re}_{ta,crit}$ varies differently with respect to $\sqrt{\omega'}$. The value of $\mathrm{Re}_{ta,crit}$ increases with increasing of $\sqrt{\omega'}$ up to $\sqrt{\omega'}$ =3.85. After $\sqrt{\omega'}$ =3.85, $\mathrm{Re}_{ta,crit}$ decreases sharply with increasing of $\sqrt{\omega'}$ in the range of 3.85≤ $\sqrt{\omega'}$ ≤12.17, however $\mathrm{Re}_{ta,crit}$ increases in the range of 12.17< $\sqrt{\omega'}$ <27.22 and then begins to decrease at $\sqrt{\omega'}$ ≥27.22.

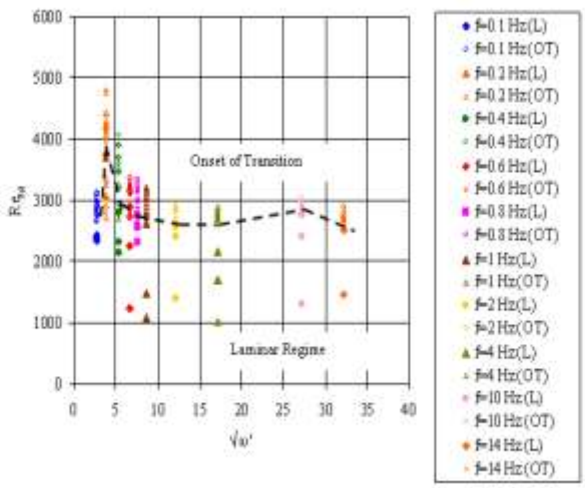

Figure 12. Flow map showing laminar regime and the onset of transition in terms of Re_{ta} and $\sqrt{\omega'}$

CONCLUDING REMARKS

Based on the presented study in this paper, the following conclusions can be drawn.

1) The onset of transition in pulsatile pipe flow is detected using an original method constructed in LabView 2009SP1®. The method operates accurately for all runs in the covered ranges of 2.72≤ $\sqrt{\omega'}$ ≤32.21 and 0.05±0.0017≤ A_1 ≤ 0.96±0.03 verifying its success and effectiveness.
2) The determination of transition onset is based on the comparisons of the magnitudes of the defined *TDP* and *TP*. The dynamic *TDP* is derived as $TDP_2 = \left[R(dU(t)/dt)^2\right] / \left[\overline{U}_{ta} \nu \omega^2\right]$ for f≤1 Hz and $TDP_3 = \left[(dU(t)/dt)^2\right] / \left[\overline{U}_{ta}^2 \omega^2\right]$ for f>1 Hz. The dynamic *TP* is derived as $TP_2 = \left(1/\sqrt{\omega'}\right)^f$ for f≤1 Hz and $TP_3 = 1/\sqrt{\omega'}^4$ for f >1 Hz.
3) The critical magnitude of f=1 Hz corresponding to $\sqrt{\omega'}$ =8.61 is also verified in conformity with the literature survey.
4) As an original contribution to the related literature, two flow maps are proposed to identify the border between laminar flow and transition onset in terms of $\mathrm{Re}_{ta} = \mathrm{Re}_{ta}(\mathrm{Re}_{os})$ and $\mathrm{Re}_{ta} = \mathrm{Re}_{ta}(\sqrt{\omega'})$ in the covered experimental range.

5) The extent of laminar flow region is roughly determined as Re_{ta} <2700 according to the constructed flow maps. This shows that the critical Re number for transition to turbulence in steady flow can be retarded to the higher Re numbers by means of the addition of oscillation to the steady flow.
6) Besides the critical values of Re_{ta} has been roughly found as $\mathrm{Re}_{ta,crit}$ =2700 for the transition onset, the magnitude of $\mathrm{Re}_{ta,crit}$ is found to vary with respect to $\sqrt{\omega'}$ as is seen in flow maps. It is apparent that $\sqrt{\omega'}$ has a strong effect on $\mathrm{Re}_{ta,crit}$.
7) The proposed methodology gives a novel contribution as well as an alternative and an accurate approach with fully-automated feature of the devised program instead of the available detection method of "visual observation of turbulence on velocity waveforms".
8) The proposed methodology should be verified for further studies. It can be used in the covered experimental ranges herein, especially in $\sqrt{\omega'}$ range, by other researchers. In the different experimental ranges, it is also possible to derive their own threshold parameter, *TP* using the same methodology, the detection procedure and the turbulence detection parameter, *TDP*.

ACKNOWLEDGEMENTS

The authors would like to thank the Research Fund of the University of Gaziantep for the research project supported under grant no: MF.09.09.

REFERENCES

Clamen M. and Minton P., 1977, An Experimental Investigation of Flow in an Oscillating Pipe, *J. Fluid Mech.*, 81, 421-431.

Çarpınlıoğlu M. Ö., 2003, An Approach for Transition Correlation of Laminar Pulsatile Pipe Flows via Frictional Field Characteristics, *Flow Meas. Instrum.*, 14, 233-242.

Çarpınlıoğlu M. Ö. and Gündoğdu M. Y., 2001, A Critical Review on Pulsatile Pipe Flow Studies Directing towards Future Research Topics, *Flow Meas. Instrum.*, 12, 163-174.

Çarpınlıoğlu M. Ö. and Özahi E., 2011, Laminar Flow Control via Utilization of Pipe Entrance Inserts (A Comment on Entrance Length Concept), *Flow Meas. Instrum.*, 22, 165-174.

Einav S. and Sokolov M., 1993, An Experimental Study of Pulsatile Pipe Flow in the Transition Range, *Trans. ASME*, 115, 404-411.

Gilbrech D. A. and Combs G. D., 1963, Critical Reynolds Numbers for Incompressible Pulsating Flow in Tubes, *Dev. Theo. Appl. Mech.*, 1, 292-304.

Gündoğdu M. Y. and Çarpınlıoğlu M. Ö., 1999, PresentState of Art on Pulsatile Flow Theory Part 1: Laminar and Transitional Flow Regimes, *JSME Int. J. Series B Fluids and Therm.Eng.*, 42, 384-397.

Hershey D. and Im C. S., 1968, Critical Reynolds Number for Sinusoidal Flow of Water in Rigid Tubes, *AIChE J.*, 14, 807-809.

Iguchi M. and Ohmi M., 1984, Transition to Turbulence in a Pulsatile Pipe Flow Part 3: Flow Regimes and the Conditions Describing the Generation and Decay of Turbulence, *Bull. JSME*, 27, 1873-1880.

Nabavi M., 2010, Invited Review Article: Unsteady and Pulsating Pressure and Temperature: A Review of Experimental Techniques, *Rev. Sci. Instrum.*, 81, 031101.

Nabavi M. and Siddiqui K., 2010, A Critical Review on Advanced Velocity Measurement Techniques in Pulsating Flows, *Meas. Sci. Technol.*, 21, 042002.

Ohmi M. and Iguchi M., 1980, Flow Pattern and Frictional Losses in Pulsating Pipe Flow Part 2: Effect of Pulsating Frequency on the Turbulent Frictional Losses, *Bull. JSME*, 23, 2021-2028.

Ohmi M., Iguchi M. and Urahata I., 1982, Transition to Turbulence in a Pulsatile Pipe Flow Part 1: Wave Forms and Distribution of Pulsatile Velocities near Transition Region, *Bull. JSME*, 25, 182-189.

Ohmi M., Iguchi M. and Usui T., 1981, Flow Pattern and Frictional Losses in Pulsating Pipe Flow Part 5: Wall Shear Stress and Flow Pattern in a Laminar Flow. *Bull JSME*, 24, 75-81.

Özahi E., 2011, *Analysis of Laminar-Turbulent Transition in Time-Dependent Pipe Flows*, Ph.D. Thesis, University of Gaziantep.

Özahi E., Çarpınlıoğlu M. Ö. and Gündoğdu M. Y., 2010, Simple Methods for Low Speed Calibration of Hot-Wire Anemometers, *Flow Meas. Instrum.*, 2, 166-170.

Peacock J., Jones T., Tock C. and Lutz R., 1998, The Onset of Turbulence in Physiological Pulsatile Flow in a Straight Tube, *Exp. Fluids*, 24, 1-9.

Sarpkaya T., 1966, Experimental Determination of the Critical Reynolds Number for Pulsating Poiseuille Flow, *Trans. ASME D J. Basic Eng.*, 88, 589-598.

Shemer L., 1985, Laminar-Turbulent Transition in a Slowly Pulsating Pipe Flow, *Phys. Fluids*, 28, 3506-3509.

Stettler J. C. and Hussain K. M. F., 1986, On Transition of the Pulsatile Pipe Flow, *J. Fluid Mech.*, 170, 169-197.

Yellin E. L., 1966, Laminar-Turbulent Transition Process in Pulsatile Flow, *Circulation Res.*, 19, 791-804.